N64-26591

Code-1   Cat. 19

nasa-JmX-53066

NASA TM X-53066

PERMEATION OF ADHESIVELY BONDED JOINTS BY GASEOUS AND LIQUID HYDROGEN

by C. T. EGGER, D. A. NAUMAN,
   T. J. CARTER, AND J. B. GAYLE
   Propulsion and Vehicle Engineering Laboratory

NASA

George C. Marshall
Space Flight Center,
Huntsville, Alabama

OTS PRICE

XEROX $ *3.60 ph.*

MICROFILM $ _____

TECHNICAL MEMORANDUM X-53066

PERMEATION OF ADHESIVELY BONDED JOINTS BY GASEOUS AND LIQUID HYDROGEN

By

C. T. Egger
D. A. Nauman
T. J. Carter
J. B. Gayle

George C. Marshall Space Flight Center

Huntsville, Alabama

ABSTRACT

$2 6 5 7 /$

The permeabilities of selected adhesives to gaseous and liquid hydrogen were determined experimentally. Frequent rupture on exposure to liquid hydrogen suggests that for the nonfilleting adhesives bond integrity rather than permeability considerations will limit the utility of adhesive bonds for liquid hydrogen applications. Permeabilities for the filleting adhesives are several orders of magnitude higher and tend to preclude their use for such applications. author

NASA-GEORGE C. MARSHALL SPACE FLIGHT CENTER

TECHNICAL MEMORANDUM X-53066

PERMEATION OF ADHESIVELY BONDED JOINTS
BY GASEOUS AND LIQUID HYDROGEN

By

C. T. Egger
D. A. Nauman
T. J. Carter
J. B. Gayle

MATERIALS DIVISION
PROPULSION AND VEHICLE ENGINEERING LABORATORY
RESEARCH AND DEVELOPMENT OPERATIONS

TABLE OF CONTENTS

LIST OF ILLUSTRATIONS

LIST OF TABLES

PERMEATION OF ADHESIVELY BONDED JOINTS
BY GASEOUS AND LIQUID HYDROGEN

SUMMARY

The permeabilities of selected adhesives to gaseous and liquid hydrogen were determined experimentally. Frequent rupture on exposure to liquid hydrogen suggests that for the nonfilleting adhesives bond integrity rather than permeability considerations will limit the utility of adhesive bonds for liquid hydrogen applications. Permeabilities for the filleting adhesives are several orders of magnitude higher and tend to preclude their use for such applications.

INTRODUCTION

The capability of adhesively bonded joints to seal the bulkhead from permeation by hydrogen is of great importance in repair procedures for the hydrogen/oxygen common bulkheads of the Saturn S-IV, S-IVB, and S-II stages. Such a sealing technique also lends itself to consideration as a contingency method for fabrication of the entire bulkhead.

This report presents the results of a two-part program to measure quantitatively hydrogen permeation through adhesively bonded joints. The first part consisted of a study of gaseous hydrogen permeation at room temperature. The objectives of this part of the study were twofold: to provide interim information for the Saturn program pending completion of the liquid phase experiments and to obtain data on which to base the design of the liquid phase experiments. The second part consisted of a study of liquid hydrogen (LH_2) permeation; the objective was to qualify adhesives for LH_2 applications.

GAS-PHASE STUDIES

Experimental

The specimens (FIG 1) consisted of annular plates, having outside diameters of 6 inches and inside diameters ranging from 0.5 to 3 inches, onto which were bonded 3.5-inch diameter discs; this provided bonded overlaps of 1.5, 1, 0.75, and 0.25 inch, respectively. Peripheral holes were provided for mounting in the flange fixture (FIG 2) used for permeation measurements.

For consistency with proposed vehicle applications, 2014-T6 aluminum (.063 inch) was used as the metal for all tests. Although literature values for aluminum and alloy permeabilities are not uniform, permeation through the aluminum portions of the test specimens was expected to be negligible when compared with that through the bonds; this was confirmed by permeability determinations on solid aluminum plates.

For prebond cleaning, the metal surfaces were degreased and then immersed for 20 minutes in a 150-160°F bath of 1 part (by weight) sodium dichromate, 3 parts concentrated sulfuric acid, and 9 parts distilled water. All surfaces then were rinsed thoroughly in distilled water and dried before bonding. The adhesives used and pertinent details such as curing conditions are listed in Table I.

All specimens were qualitatively checked for bond integrity using a helium mass spectrometer leak detector and then were conditioned for at least 12 hours at a pressure less than 10^{-4} Torr. Runs were made at the prevailing laboratory temperatures which varied from approximately 23° to 28°C.

Three methods of flow measurement were employed: (1) hydrogen permeation using a CEC Model 620 mass spectrometer, (2) helium permeation using the Veeco MS-9ABC helium mass spectrometer leak detector, and (3) helium permeation using the Major Model A-6 pressure rise volumetric permeation instrument. All specimens were run by each of the three methods, but some exhibited too rapid a flow for detection on the Veeco instrument, and others were too impermeable to yield significant results on the Major system.

Two modes of operation were required on the mass spectrometer, depending upon the volumetric rate of flow for the specimen being tested:

a. Accumulation of gas permeating over a timed interval was required for those specimens passing the least amount of hydrogen.

b. Ordinary mass spectrometric analysis was not possible for the specimens of greatest permeability; for those specimens, flow rates were estimated from the rate of pressure rise in the accumulation chamber of the spectrometer.

In general, the experimental arrangement was as shown in FIG 3. The permeating gas was passed over the upstream face of the specimen at a pressure not more than 0.5 centimeter of water greater than atmospheric. The permeating gas passed into a chamber of relatively zero pressure which was connected to the mass spectrometer for quantitative rate measurement. It should be noted that, even for those runs where accumulation or pressure rise was employed, the downstream pressure did not rise to more than 0.1 percent of the pressure upstream of the adhesive bond. Therefore, all pressure drops were taken as equal to observed barometric pressure.

Except for very permeable specimens requiring pressure-rise measurement, all samples were exposed to the experimental conditions for at least one hour before rate measurement. Determinations then were made at selected intervals until a constant rate was attained. In no case was more than 15 hours required for disappearance of transient behavior.

Safety precautions included elimination of leaks from the upstream hydrogen chamber, careful minimizing of the hydrogen flow (which was vented outside the building), and constant monitoring of the laboratory atmosphere for ambient hydrogen.

The results are given in Table II and presented graphically in FIG 4 through 7. Figures 4 and 6 present the data in terms of measured

flow rates, and FIG 5 and 7 present the same data after reduction to permeability units, SPU.*

As indicated in the figures, several of the HT-424u and Aerobond 430 data points represent flows in excess of the measurable limit so the ranges shown for those adhesives should be regarded as the lower end of the true spectra.

Discussion of Gas Phase Results

Experimental errors in the determination of the flow rates for any given specimen are thought to be small; thus, pressure measurements should not contribute errors in excess of 1 percent. Physical specimen measurements could contribute errors up to 20 percent because of the non-uniformity of the bond thickness, but multiple determinations were made and averaged which probably reduced the error to less than 7 percent. Mass spectrometer errors should not exceed 10 percent; however, for those samples requiring pressure rise measurements, errors of up to 20 percent are probable. Therefore, the overall variability of the determinations would be expected to amount to roughly 30 percent. Support for this estimate is provided by hydrogen permeability results (Table II) for specimens for which duplicate determinations were made. Of the 14 pairs of results, deviations of the individual values from the average values exceeded 30 percent in only 3 instances, and 2 of these probably were the result of damage to the adhesive bonds because of repeated handling between determinations. (In all cases, the reruns were made at least 90 days after the original measurement.)

The estimated 30 percent variability associated with the permeability measurements may be compared with the much larger variability noted for permeability of duplicate specimens. Thus, inspection of the results for the individual specimens of each adhesive indicates that the ratios of highest to lowest hydrogen permeability values ranged from a factor of approximately 4 for Narmco A to several orders of magnitude for the other adhesives. Similar results were noted for helium permeabilities. These wide variations reflect basic differences in the permeabilities of

---

* One permeability unit (SPU) is defined as the number of cubic centimeters of a gas at STP (0°C, 1 atma) passing through one square centimeter of material, one centimeter thick, under a pressure gradient of one centimeter Hg (10 Torr), in one second. Thus, the equivalent units are: 1 SPU = 1 cm^3 (STP) $\cdot$ $sec^{-1} \cdot$ cm $\cdot$ $cm^{-2} \cdot$ $(cm\,Hg\,\Delta\,P)^{-1}$.

duplicate specimens from a single adhesive. Whether such differences are inherent in adhesively bonded joints or whether they indicate a need for better quality control has not been established.

Narmco A exhibited the lowest hydrogen permeability of the adhesives tested. Thus, the initial values for all specimens were in the 10^{-12} SPU range. This adhesive also exhibited the lowest data scatter as indicated above.

Hydrogen permeabilities for the other three nonfilleting adhesives were similar with values generally falling in the 10^{-11} SPU range. However, the data scatter for these adhesives was much larger and increased in the order FM-1000 < Narmco C < BR-92.

Hydrogen permeabilities for the filleting adhesives were several orders of magnitude greater than those for the nonfilleting adhesives. Values for X-424 and HT-424 were in the 10^{-4} to 10^{-8} SPU range. Average values for HT-424u and Aerobond 430 were not determined precisely because some of the flow rates exceeded the limits of detection; however, they were greater than 10^{-3} SPU.

Inspection of the flow rates and permeabilities for helium indicates trends which are very similar to those determined for hydrogen. Collectively, the results indicate marked differences in the permeabilities of the filleting and nonfilleting adhesives. Results of previous studies on a number of polymeric materials in this laboratory suggest that permeabilities for the adhesives without mechanical flaws should be in the range of 10^{-12} to 10^{-10} SPU. Departure of observed values from these expected baseline levels indicates structural problems of an unknown nature; conversely, clustering of the lower values for the nonfilleting adhesives tends to confirm the existence of such baseline permeability minima.

An attempt was made to obtain additional information regarding the nature and extent of mechanical leaks by inspection of broken adhesive bonds. FIG 8 shows broken bonds for six adhesives. As expected, the appearance of the nonfilleting adhesive surfaces is smoother in texture than that of the filleting adhesives which normally are used with scrim cloth. However, even the nonfilleting adhesive surfaces generally are nonuniform, and, in particular, the surface of FM-1000 exhibits a distinct pattern of oblong holes which are probably caused by bubbles formed during the curing process.

Examination of FIG 4 through 7 reveals a trend toward greater flow and greater permeability with increasing adhesive overlap length, a result contrary to that expected. The physical significance of this trend is not immediately evident. Thus, there is no apparent reason why the larger bond overlaps should be generally more susceptible to mechanical leakage for both the filleting and nonfilleting adhesives. Studies of the size distribution and orientation of discontinuities within adhesive bonds as a function of overlap would be of interest in this connection.

To determine if the relatively high permeabilities of the filleting adhesives were due to the use of a fiberglass scrim cloth, a set of HT-424 specimens were prepared without the scrim cloth. The permeabilities of these specimens (designated HT-424u) were generally higher than those for the same adhesive with the scrim cloth. Therefore, it appears that the high permeabilities for the filleting adhesives must be due to the nature of the adhesives themselves rather than to channeling of gas along the fibers of the glass cloth.

Attempts were made to correlate bond thicknesses with flow rates and permeabilities for each adhesive. Although some apparent correlations were noted for specific adhesives, the data scatter was large, and the trends varied from one adhesive to another. Therefore, it is concluded that, although bond thickness may influence the permeability of a particular adhesive, the relation between these variables is obscure, and no overall correlation of the data is possible.

LIQUID-PHASE STUDIES

Experimental

The objective of this phase of the study was to qualify adhesives for use in contact with LH_2 for bulkhead patching. Therefore, only adhesives exhibiting good strength at cryogenic temperatures were studied.

Several methods for determining the permeation of LH_2 through adhesives were considered. The permeation rate determined from the patch specimens for the nonfilleting adhesives was so low that it was desirable to use some method in which the adhesive area could be greatly increased to obtain more meaningful data. This was accomplished by making permeation cells of multiple layers of adhesive

6

and flat aluminum rings (3-1/2 inches I. D. x 6 inches O. D. x .064 inch thick). The rings were bonded to each other with the test adhesive and were fitted with a bottom and a top to form a closed cell 74 layers in height. The resulting effective bond line length of approximately 90 feet yields a result which is statistically more significant in relation to bulkhead fabrication than a single bond such as in the patch specimens. The top of the cell had a 3/4-inch O. D. tube welded to it so the cell could be continuously evacuated (FIG 9)*. A Veeco mass spectrometer helium leak detector was modified to detect and record permeating hydrogen. The permeation cell was connected to the hydrogen detector through 3/4-inch tubulation containing the necessary valves (FIG 10). The hydrogen background for the modified leak detector was high, which was thought to be caused by inadequate cold trapping over the oil diffusion pump. Because this background was variable, a valve was placed in the tubulation as close to the cell as possible to obtain a true permeation rate for the cell. During a test run, this valve was opened and closed several times to determine the portion of the total rate which was due to permeation into the cell.

A facility designed for hazardous experiments was used for all LH$_2$ testing. The instrumentation was housed inside the structure, which had a 3/8-inch thick steel wall; the cryostat and storage dewars were located outside (FIG 11 and 12). The cryostat was a completely sealed container except for a line that provided venting to the air, ten feet above ground. The equipment was arranged so that all controls were remotely operated when LH$_2$ was used. Precautions were taken to exclude hydrogen gas from reaching any part of the leak detector except through the vacuum tubulation. The instrument had an automatic valve-closing feature which isolated the permeation cell when the cell pressure rose above 3×10^{-4} Torr. Other major items of equipment of an auxiliary nature were 100-liter LN$_2$ and LH$_2$ dewars, a liquid cryogen level-controlling recorder, and a 0-10 millivolt recorder for recording leak detector output.

Each cell was leak checked with helium at room temperature and again while cold (immediately after being removed from a LN$_2$ bath) to find mechanical leaks around welds and any obvious leaks in the

---

* During fabrication, the cell tops were installed last; then the pump-out tubulation was welded to the tops. The tops were originally made of stainless steel for ease in welding; however, the material was changed to 2014-T6 aluminum alloy after several tops popped off during welding on the BR-92 cells, probably because of the difference in expansion of the materials and the brittle nature of the adhesive.

adhesive bonds. After sealing all leaks, the permeability to gaseous hydrogen was determined at ambient temperature for most of the cells.* This was accomplished by enclosing the cell in a container (FIG 13), outgassing the cell and container for about 24 hours in a vacuum, and then filling the enclosing container with hydrogen gas. After the cell had come to equilibrium, the hydrogen permeation rate was determined by opening and closing the cell valve as described above. Gaseous hydrogen permeabilities are summarized in Table III.

Permeation of liquid hydrogen was determined in much the same manner as for gaseous hydrogen except that the enclosing container was much more elaborate. For these tests, the permeation cell was placed into a triple-walled cryostat and evacuated until the background became reasonably constant, usually 16-18 hours or overnight. The cryostat and cell were then precooled with LN_2, and the cell background was determined. The LN_2 precoolant was removed, and the cryostat was filled with LH_2 to a level sufficient to cover the cell. The LH_2 level was controlled with a copper-constantan thermocouple connected through a controlling recorder to a cryogenic solenoid valve. Hydrogen permeation into the cell was determined as before by manipulation of the valve in the cell tubulation.

The hydrogen detector was recalibrated periodically by using a previously-calibrated hydrogen source which was placed in the system tubulation as close to the cell as possible to simulate hydrogen originating in the cell. During calibration, the detector appeared to be slightly less sensitive to hydrogen while the cell was immersed in LH_2, probably because of cryopumping of extraneous gases in the cell and trapping of some hydrogen by the cryopumped gases. For this reason, the cell was not closed off from the system during calibration; instead, the calibration rate was determined by noting the difference in rates with and without the standard hydrogen source connected to the system.

The results are included in Table III. Inspection of the data indicates that all hydrogen flow rates were either above the maximum (1.8×10^{-5} cc STP/sec) or below the minimum (4.5×10^{-8} cc STP/sec) of the detectable hydrogen range of the modified leak detector. Therefore, all permeability values in the table were calculated from these minimum and maximum detectable flow rates and the total adhesive thickness of the individual cells.

---

* Some of the cells were not complete when the hydrogen detector was moved to the LH_2 test facility; GH_2 permeability determinations were not made on these cells before LH_2 testing.

Exposure times in LN_2 and LH_2 are given in FIG 14 and 15.

After completion of LH_2 testing, those cells which remained intact were again checked with gaseous hydrogen. The results are included in Table III.

Ruptured cells were leak checked with helium to determine where the rupture occurred. No significant outward change in the cells was noted. Helium leak checking showed no detectable leak in the FM-1000-1 or Narmco C-2 or -3 cells at room temperature. The Narmco C-1 cell leaked at the bond between the top and the cell. This cell had a stainless steel top which was attached before fabrication trouble was experienced with BR-92 cells. BR-92 cells appeared to have suffered multiple fracturing under cold shock, resulting in gross leakage through the cell walls at numerous locations.

No attempt was made to conduct LH_2 permeation studies on the filleting adhesives because of the high permeabilities found during the gaseous studies on single bonds. Flow rates for cells using these adhesives would be expected to exceed the upper limit of hydrogen detection on the Veeco leak detector. However, liquid nitrogen permeation rates for cells using these adhesives were determined by pressure-rise experiments in liquid nitrogen by evacuating the cells while immersed and recording the pressure rise after valving off the vacuum pump. Rate of pressure change, at a given time and pressure level, permitted calculation of the LN_2 permeability values shown in Table IV.

Discussion of Liquid Phase Results

All adhesives tested had an initial LH_2 permeation rate lower than that detectable by the modified leak detector. However, many of the cells appeared to rupture shortly after immersion in LH_2, whereupon the hydrogen flow rates increased to values in excess of the upper limit of quantitative measurement. These ruptures were all similar in character but varied in apparent magnitude and in the length of time in LH_2 before occurring. A typical cell would appear to cool satisfactorily in LH_2, and the hydrogen flow rate would stabilize; then, abruptly, the hydrogen indicator would go full scale, and the pressure gauge would show an increase that usually was enough to cause the leak detector to automatically close itself off from the cell. This

9

would require a pressure increase from 10^{-6} Torr or lower to approximately 3×10^{-4} Torr (measured at the mass spectrometer). Pressure measurement on the cell side of the automatic valve (FIG 12) generally showed an increase to above 1,000 microns, and, in some cases, the pressure rise was rapid enough to cause gurgling of the mechanical vacuum pump before the automatic valve could close. In a few of the less severe cases, continuous pumping of the cell with an auxiliary 5 cfm pump after the rupture would allow a vacuum of between 150 and 1,000 microns to be maintained. The flow of hydrogen into the auxiliary pump was evident from the pump noise which was of higher pitch than that usually noted for air. During this rough-pumping, the automatic valve remained closed, precluding quantitative measurement of hydrogen.

The behavior of the second run on the Narmco C-2 cell deserves special mention. The precool was begun at 9:30 a.m. Because there was insufficient LN_2 available to complete the precool cycle, the LH_2 fill was started at 11:20, and complete cooling was attained. The run appeared normal until 12:32 p.m. when the pressure rose abruptly to above 100 microns, causing the instrument to automatically close the tubulation to the cell. The cell was rough-pumped with the auxiliary pump to about two microns and recoupled to the instrument. Thirteen minutes later, the pressure had dropped to the 10^{-6} Torr range (measured at the mass spectrometer), and the hydrogen level was within the detectable range. In the following seven minutes, both the hydrogen flow rate and the pressure began to rise at an increasing rate. By 1:03 p.m. the cell appeared to have ruptured, the cell pressure increasing to 150 microns. By rough-pumping the cell, it was again possible to reconnect it to the instrument measurement system. This cyclic behavior was continued through 5 cycles at about 15-minute intervals before terminating the test. Although the reason for this unusual behavior has not been established definitely, results of previous investigations have indicated that liquid hydrogen permeating small leaks into an evacuated system will undergo evaporative freezing. Under these conditions, resulting solid hydrogen may form a plug sealing the leak temporarily until sufficient heat transfer takes place to melt the plug. Then, the cycle will be repeated.

Only 4 of the 12 cells using the nonfilleting adhesives survived the repeated exposures to LH_2 and LN_2 without rupturing. These included two cells each for Narmco A and FM-1000. Permeabilities for these

cells were consistently below 10^{-9} SPU. Similarly, low permeability values were determined for the other cells with nonfilleting adhesives until rupture of the cells occurred on prolonged or repeated exposure to cryogenic temperatures. Whether rupturing of adhesive bonds at liquid hydrogen temperatures is characteristic of the particular adhesives tested has not been determined. Certainly, control of temperature and pressure during bonding and also of the resulting bond thickness was unusually difficult for the multi-layered specimens. Further studies of this type using a single bond line are needed.

Liquid nitrogen permeabilities for cells with filleting adhesives were several orders of magnitude greater than the permeabilities for cells using the nonfilleting adhesives. This finding is consistent with results of gaseous permeabilities for the patch specimens.

SUMMARY AND CONCLUSIONS

The permeabilities of selected adhesives to gaseous and liquid hydrogen were determined experimentally. Frequent rupture on exposure to liquid hydrogen suggests that for the nonfilleting adhesives bond integrity rather than permeability considerations per se will limit the utility of adhesive bonds for bulkhead fabrication and repair. Permeabilities for the filleting adhesives are several orders of magnitude higher and tend to preclude their use for such applications.

For the configurations and exposure times used in this investigation, Narmco A appeared most satisfactory; however, FM-1000 gave similar results except that the gaseous permeabilities were slightly higher.

Attempts to analyze the data in terms of flow mechanisms and physical parameters were generally unsuccessful and indicated the need for additional work in this area.

2014-T6 ALUMINUM BONDED PATCH

2014-T6 ALUMINUM PLATE WITH HOLE

(SPECIMEN SHOWN APPROXIMATELY FULL SCALE)

ADHESIVE BOND

HOLE
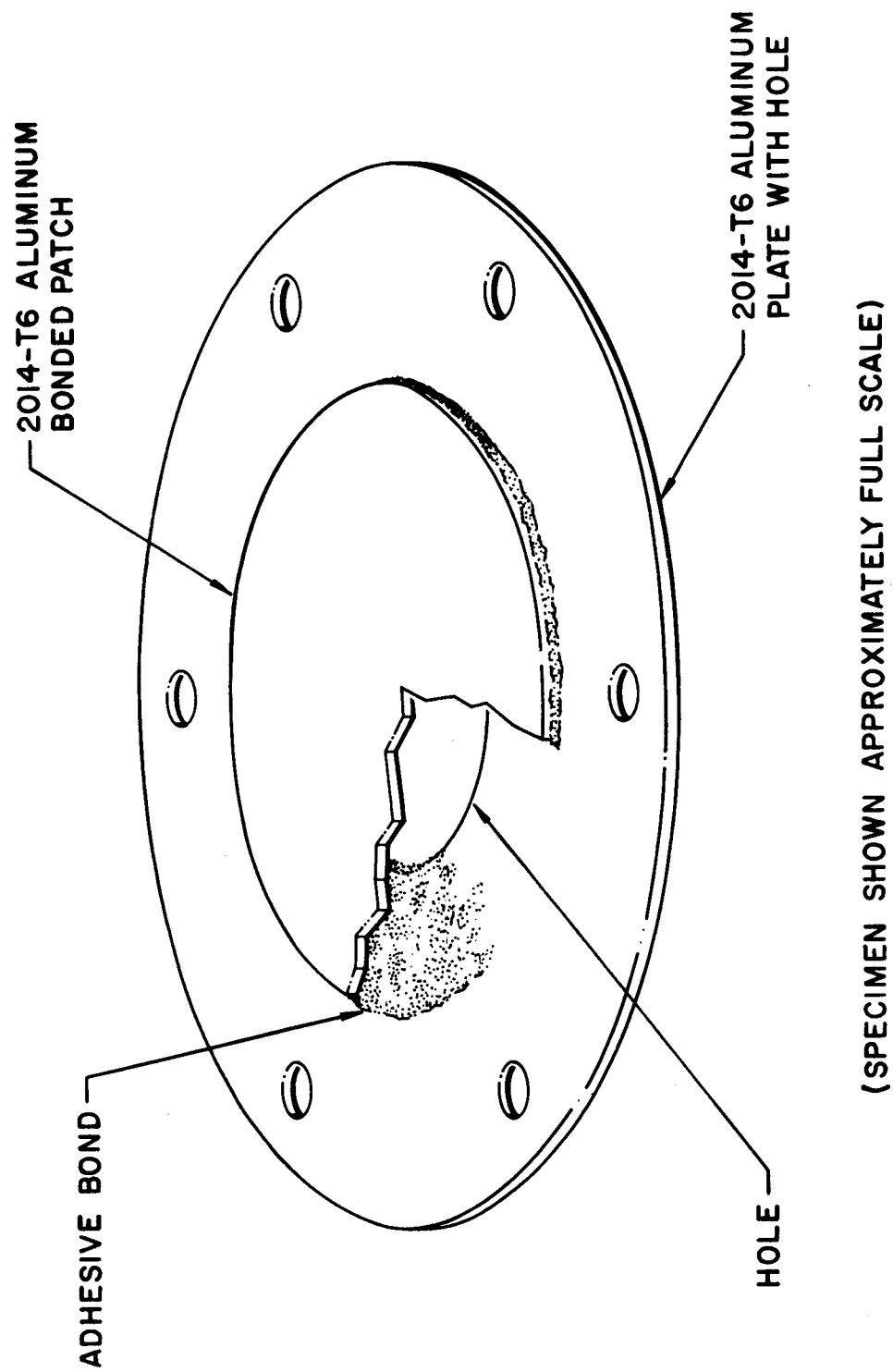
FIGURE 1.   DETAILS OF PATCH SPECIMENS

GAS INLET ──────────→   GAS OUTLET

LEAK RATE DIAPHRAGM   O-RING SEAL

THERMOCOUPLE GAUGE   MASS SPECTROMETER ADAPTER FLANGE
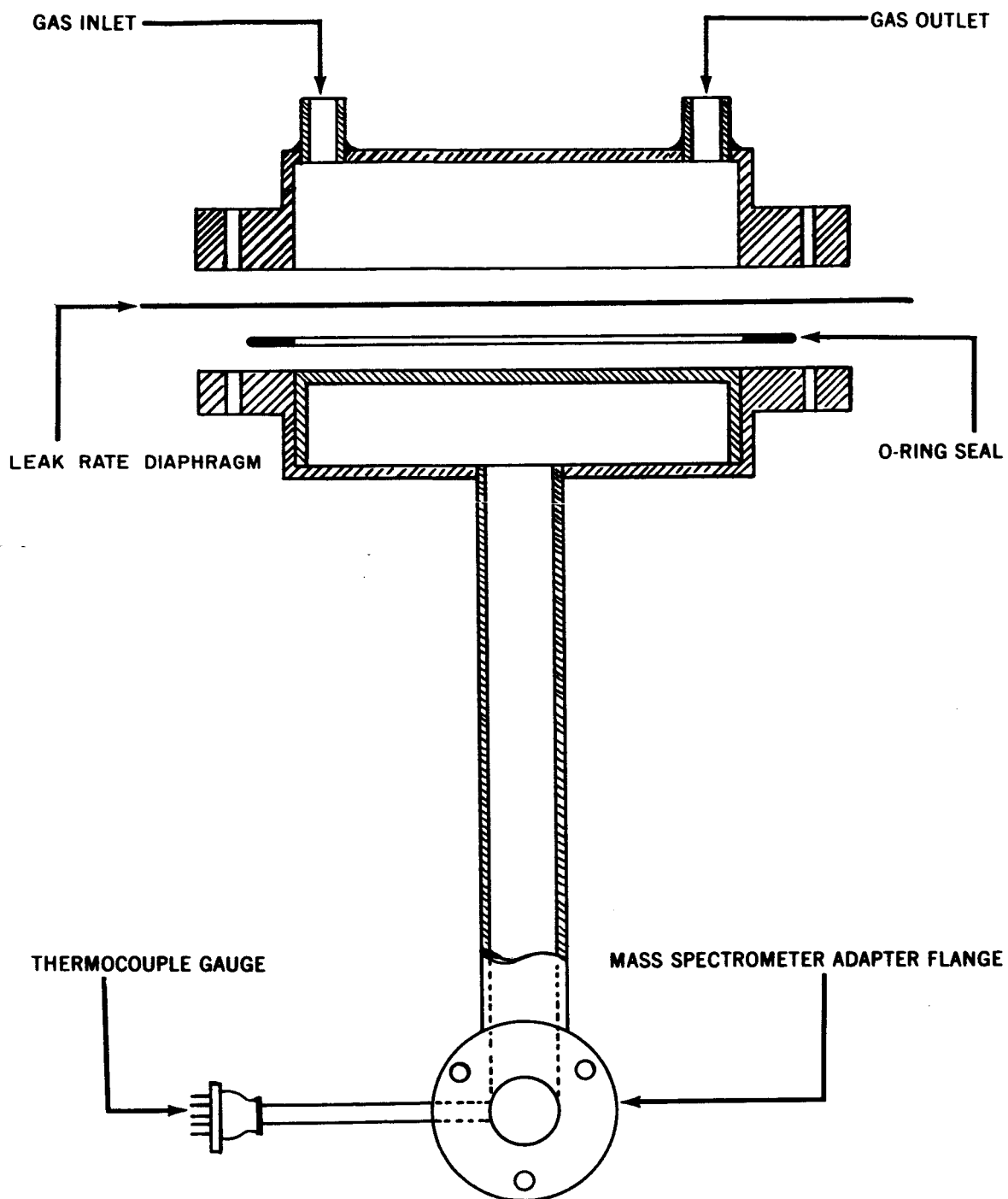
FIGURE 2. SIDE VIEW OF LEAK RATE APPARATUS
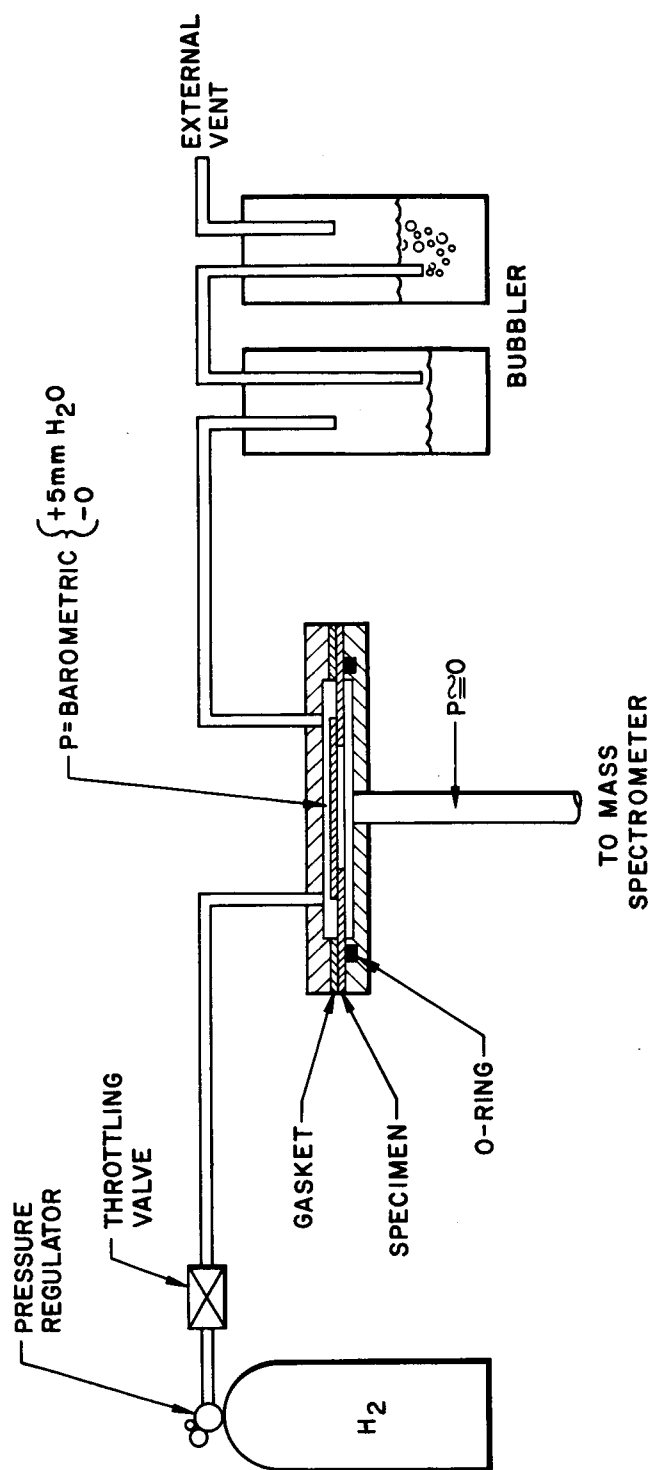
FIGURE 3.   MASS SPECTROMETRIC LEAK RATE APPARATUS
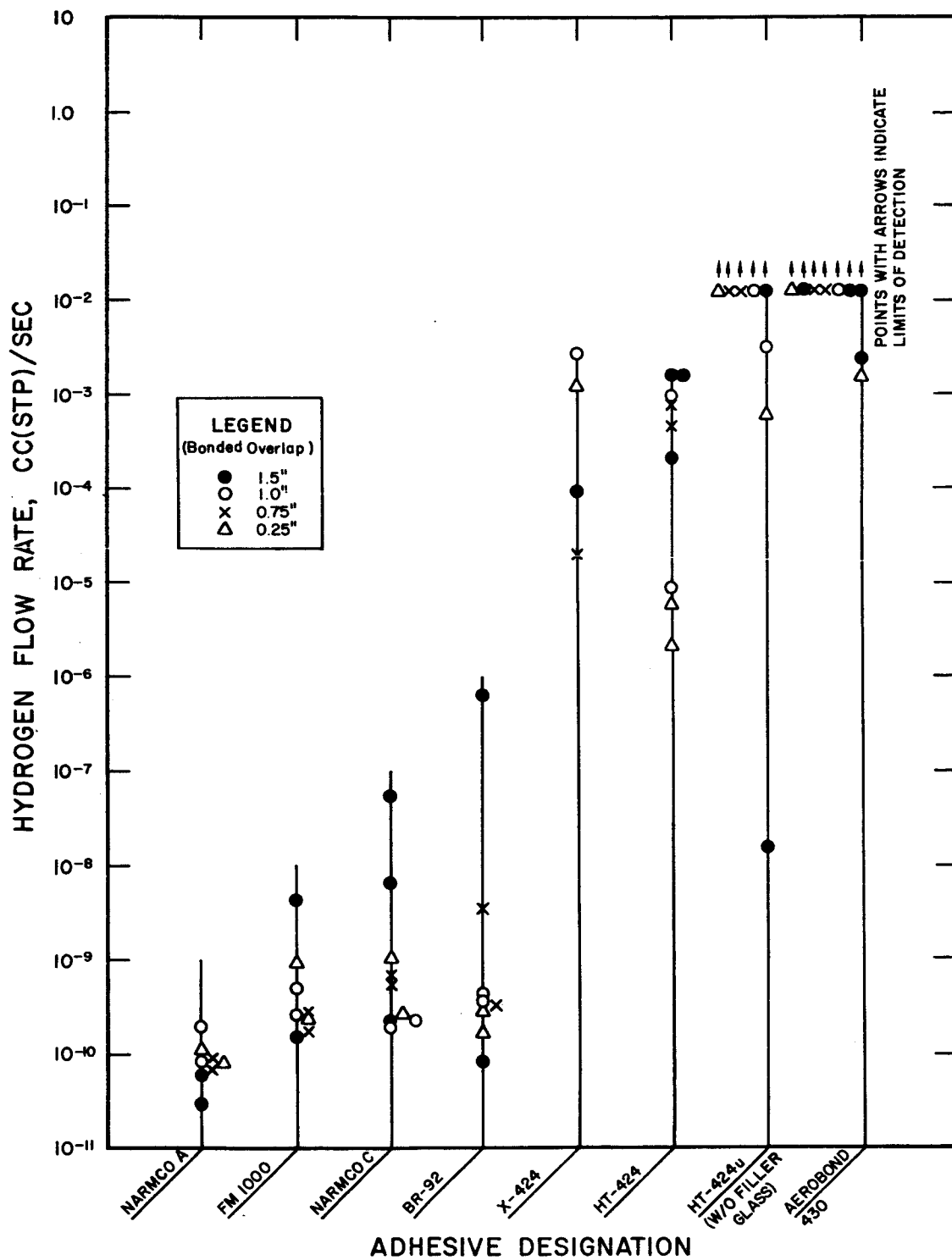
FIGURE 4. HYDROGEN FLOW RATES FOR PATCH SPECIMENS
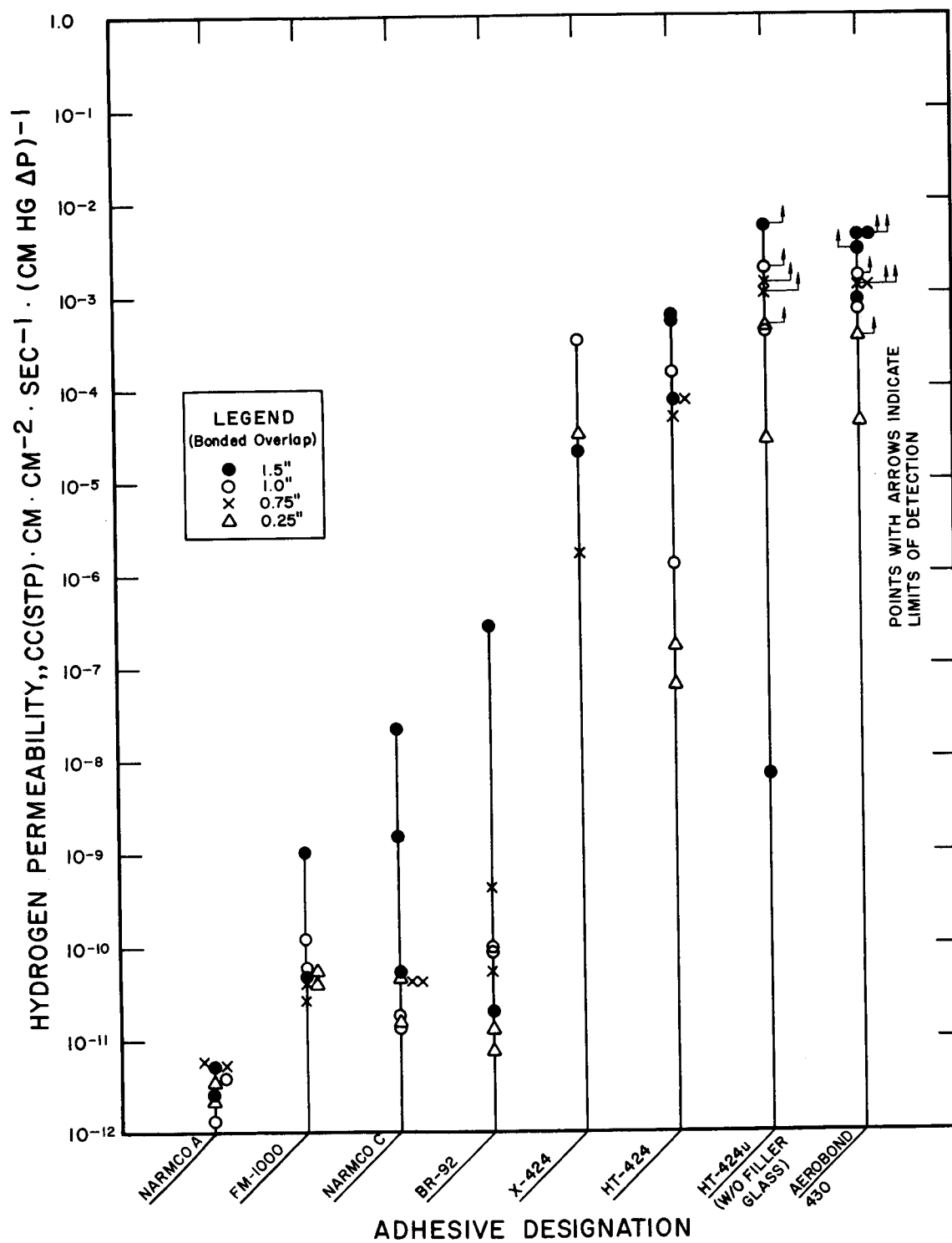
FIGURE 5. HYDROGEN PERMEABILITIES FOR PATCH SPECIMENS
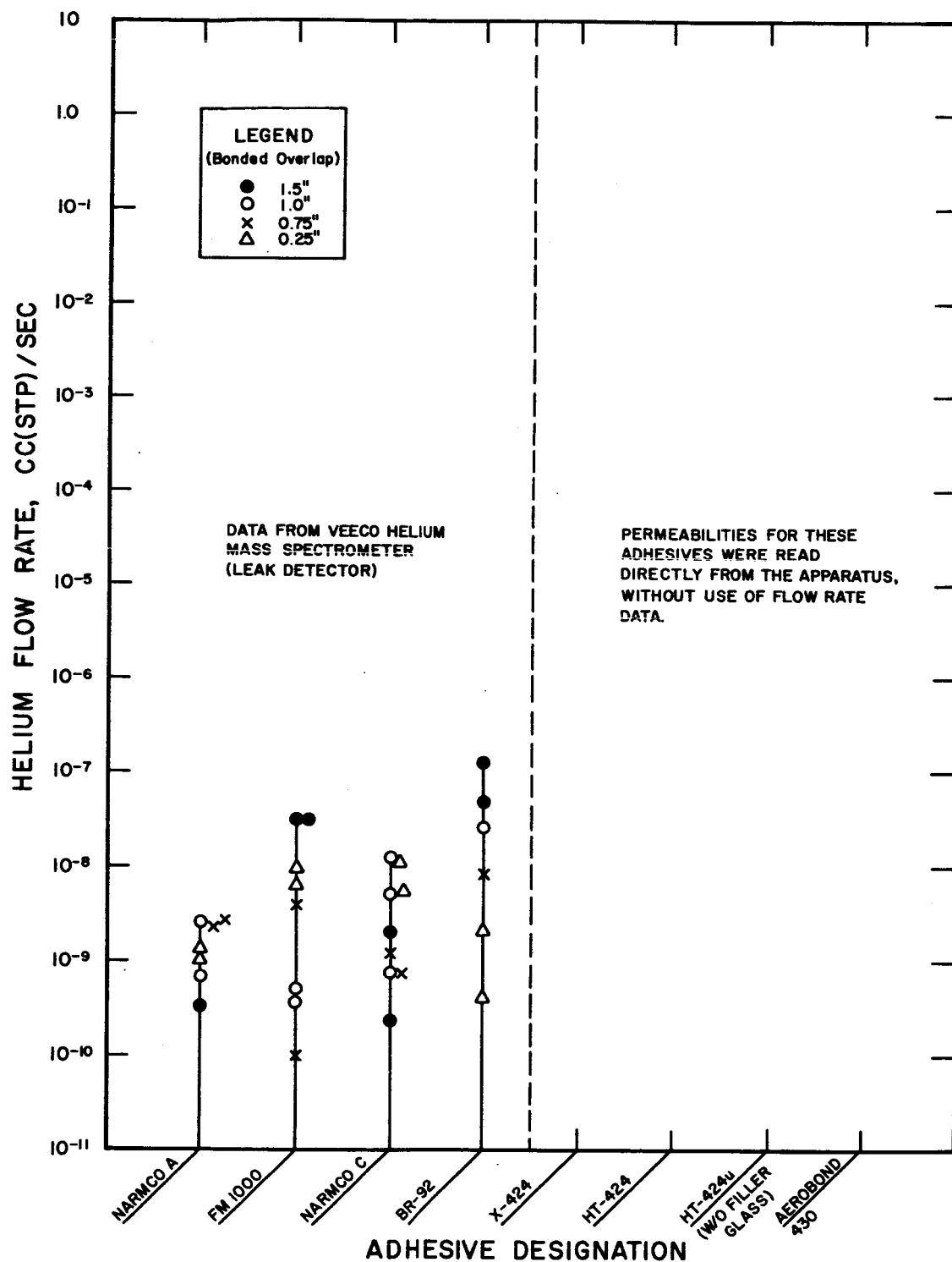
FIGURE 6. HELIUM FLOW RATES FOR PATCH SPECIMENS
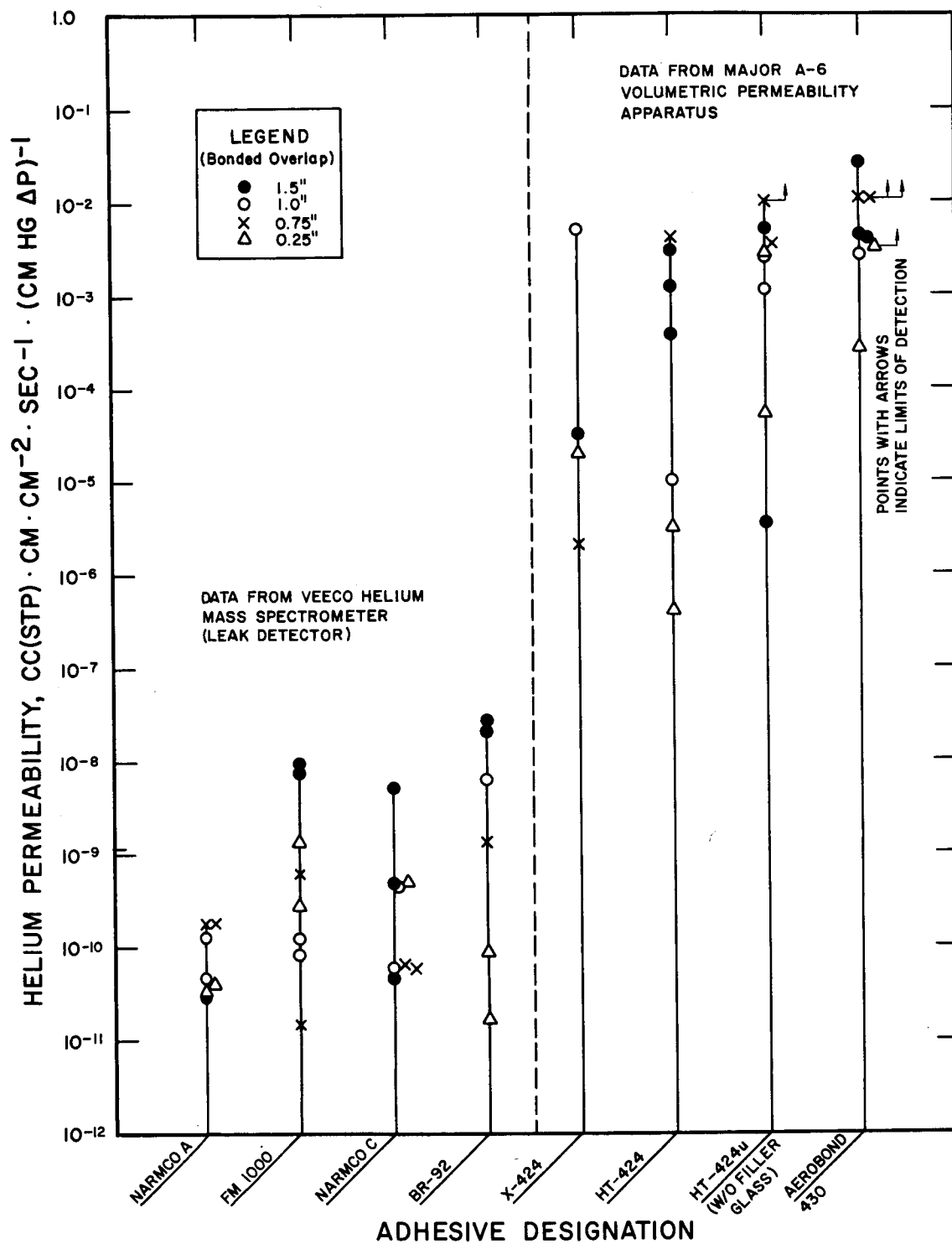
FIGURE 7. HELIUM PERMEABILITIES FOR PATCH SPECIMENS
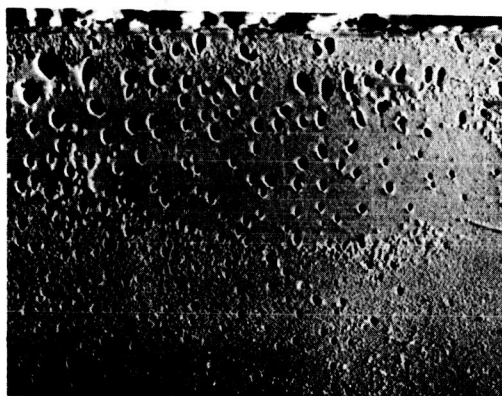
FM - 1000

BR - 92

NARMCO A

NARMCO C

HT - 424
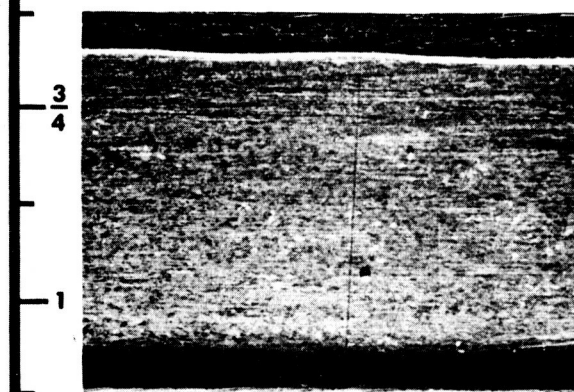
AEROBOND 430

COMPARISON OF ADHESIVES

FIGURE 8.   BROKEN ADHESIVE BONDS

FIGURE 9. LH₂ PERMEATION SPECIMEN
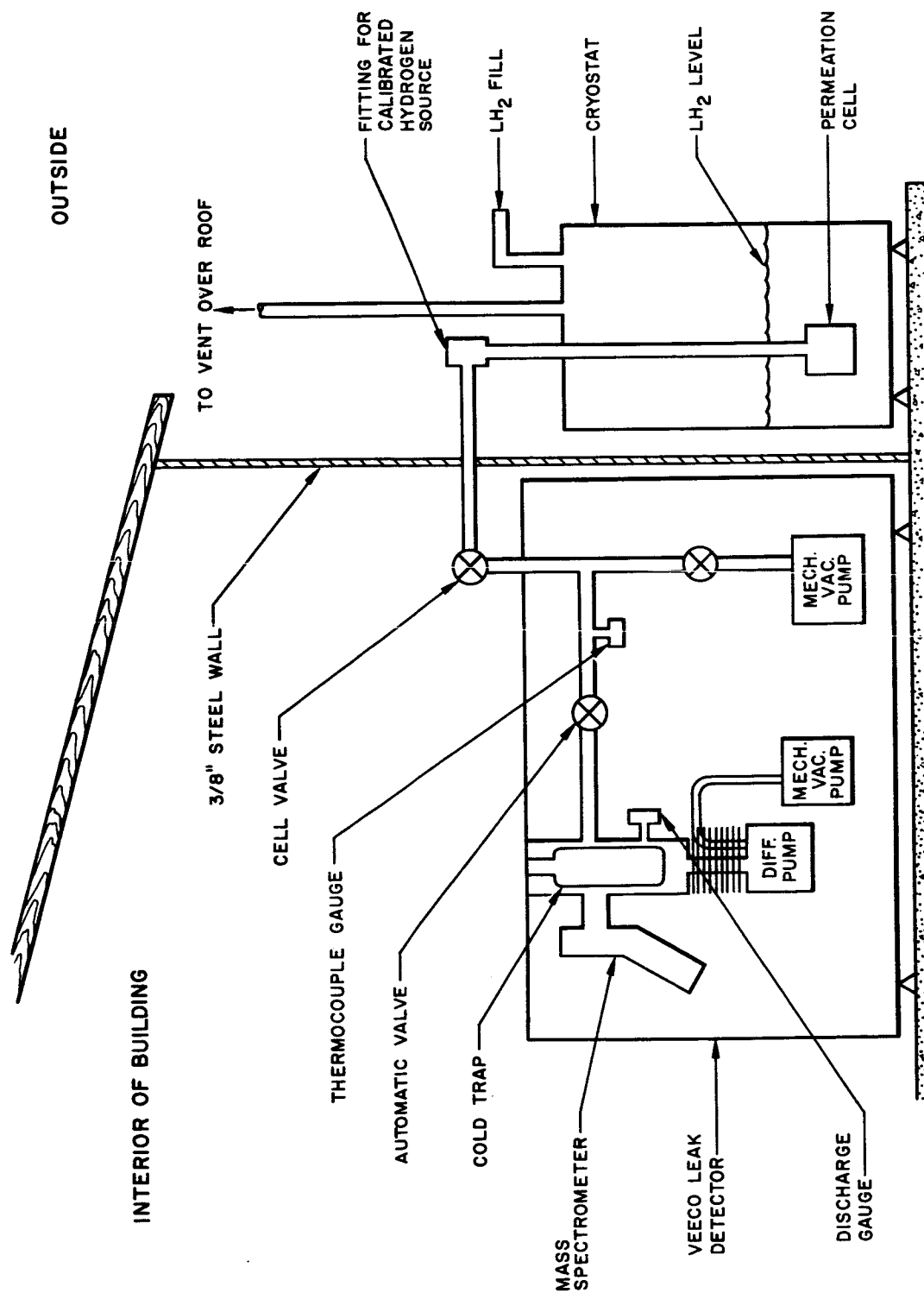
FIGURE 10. DETAILS OF LH$_2$ PERMEATION APPARATUS
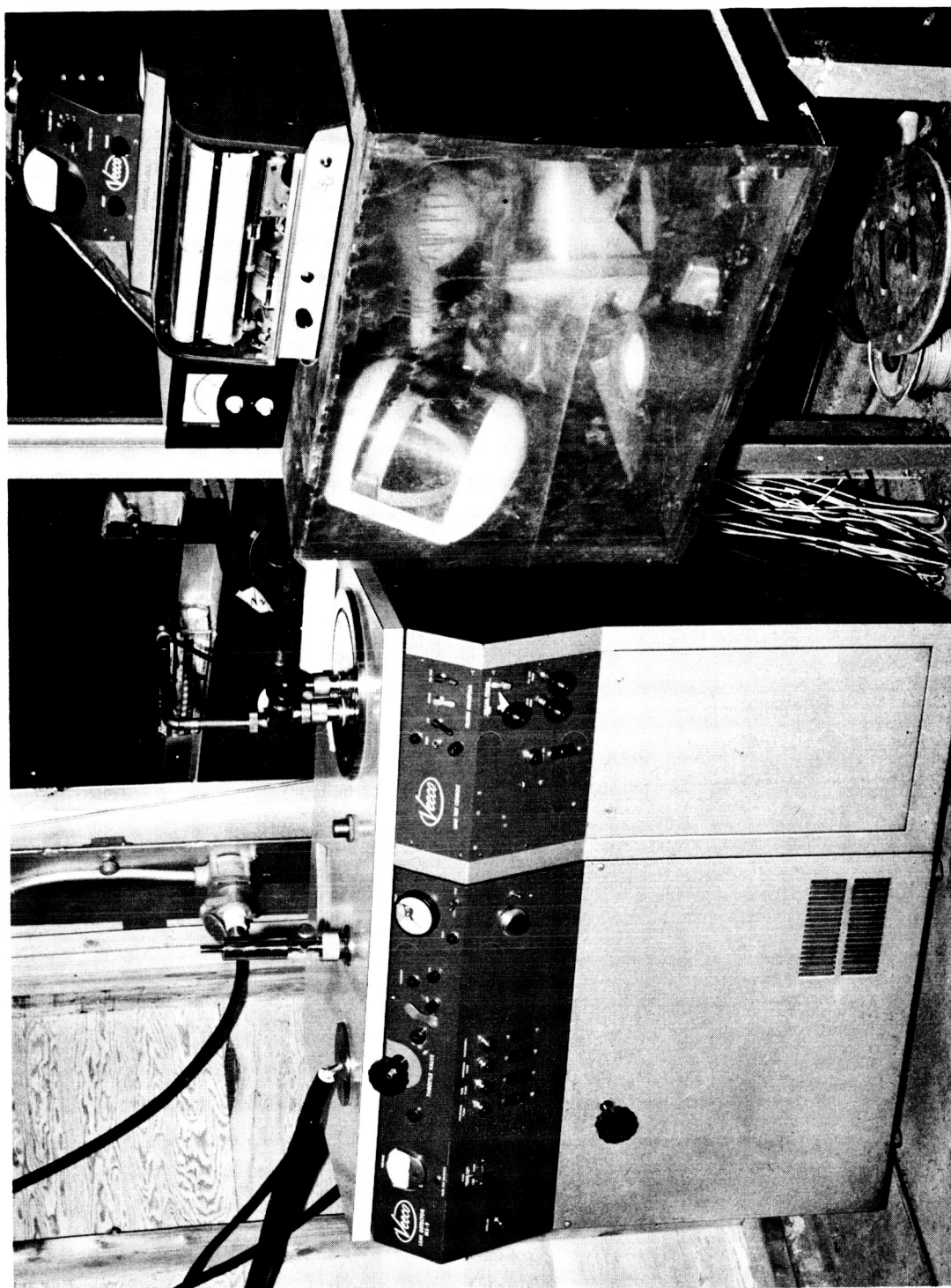
FIGURE 11.   HYDROGEN DETECTOR
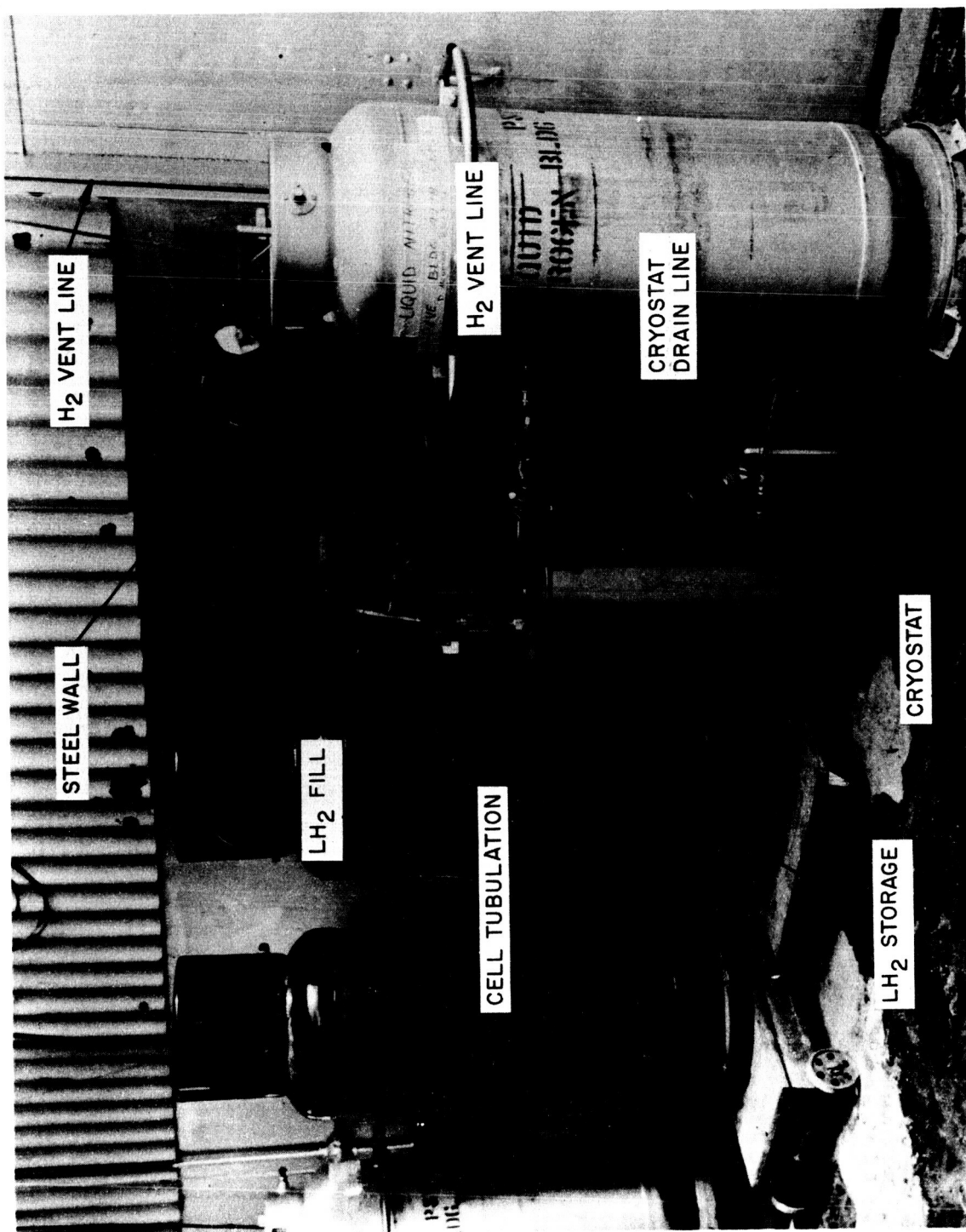
FIGURE 12. LH₂ AND LN₂ DEWARS
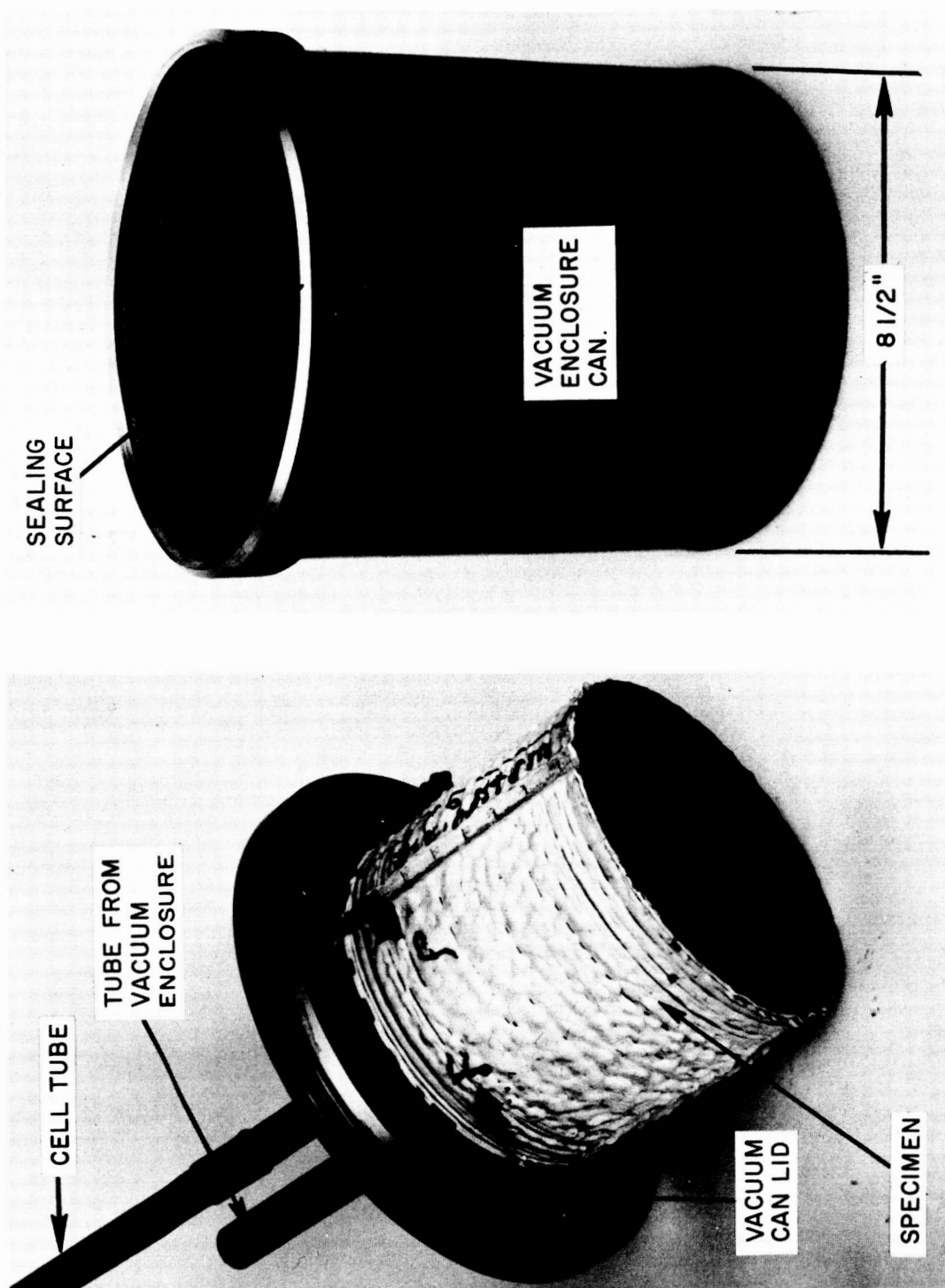
FIGURE 13.   LH$_2$ PERMEATION SPECIMEN AND CONTAINER
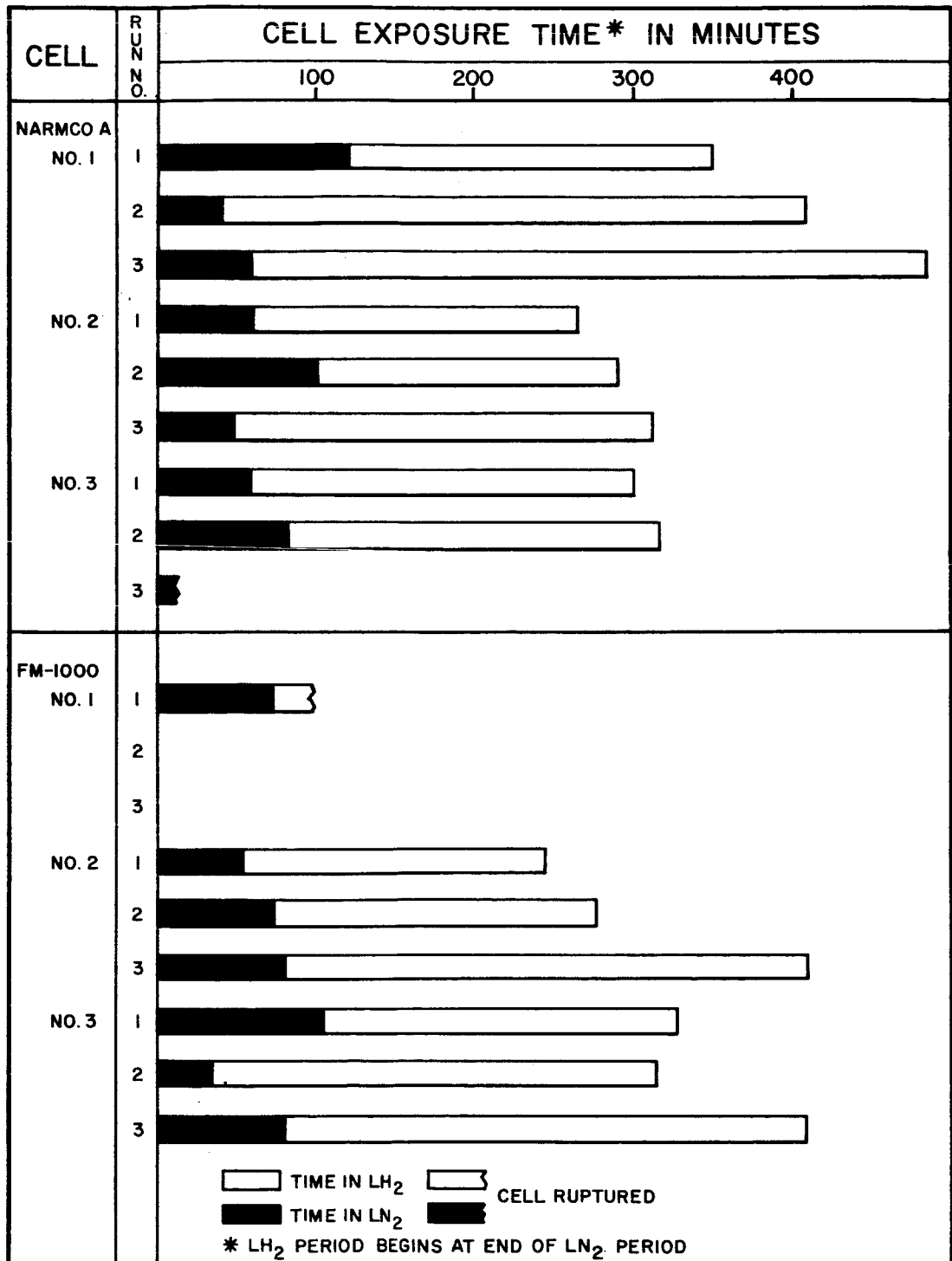
FIGURE 14. EXPOSURE HISTORIES FOR NARMCO A
AND FM-1000 CELLS
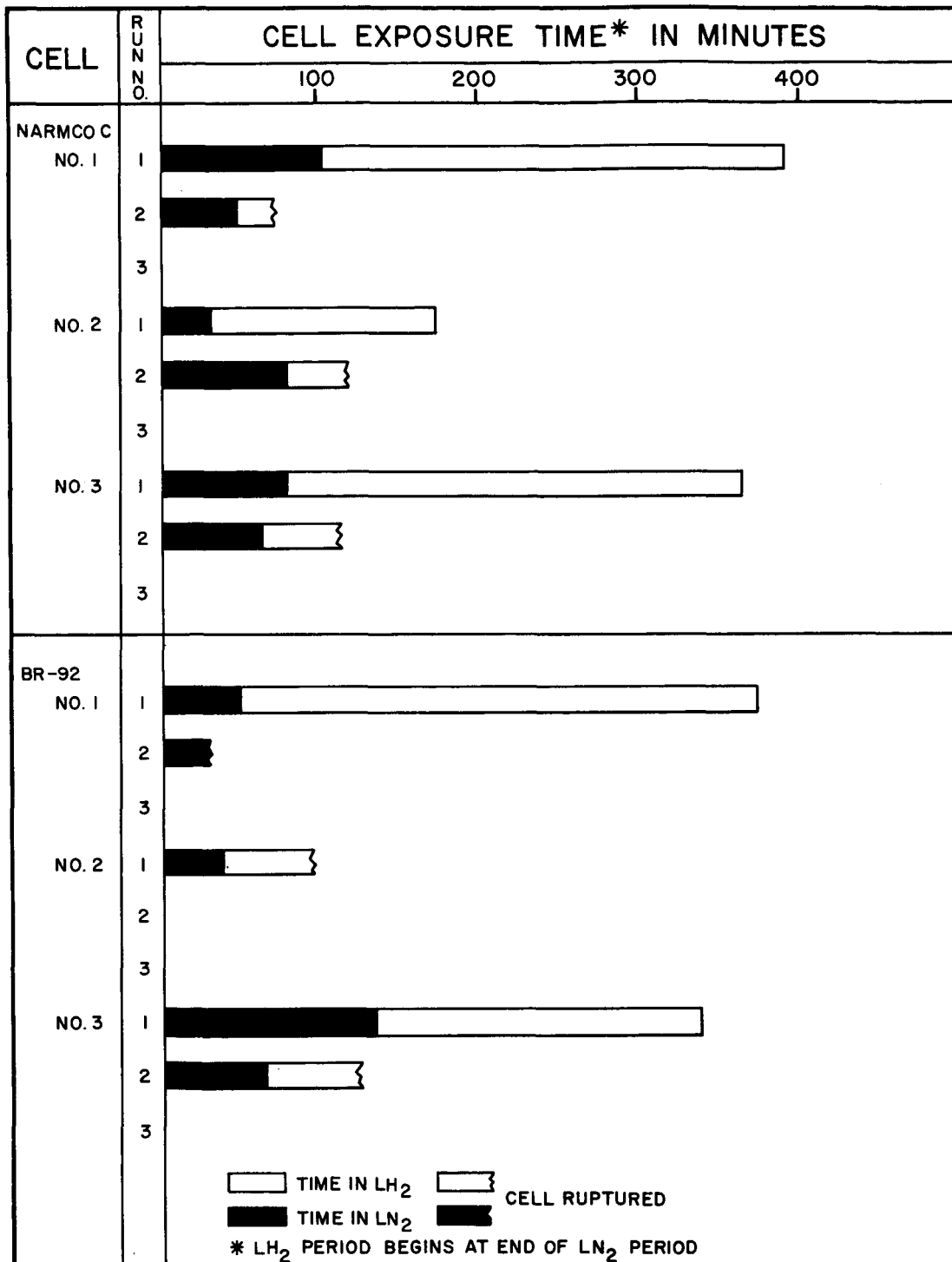
FIGURE 15.   EXPOSURE HISTORIES FOR NARMCO C
AND BR-92 CELLS

TABLE I

ADHESIVE CHARACTERISTICS

Adhesive	Type	Source	Storage Temp., °F	Filler	Raw Film Thickness, Inches	Cure Data: Time, Hours	Temperature °F	Pressure, PSIG
(Nonfilleting)								
BR-92	Epoxy, Amine Cured	Bloomingdale Rubber	<77	Unknown	Fluid, not a film	1.5	200	Contact Only
FM-1000	Epoxy, Heat Cured	Bloomingdale Rubber	<77	Nylon	0.010	1.0	350	25
Narmco A	Epoxy, Amine Cured	Narmco Materials	<77	Nylon	Fluid, not a film	<24	Ambient	Contact Only
Narmco C[1]	Polyurethane, Moca Cured	Narmco Materials	<77	Nylon	Fluid, not a film	<72	Ambient	Contact Only
(Filleting)								
Aerobond 430[2,3]	Epoxy Phenolic, Heat Cured	Adhesive Engineers	<0	Aluminum	0.015	0.67	340	25
X-424[2,3]	Epoxy Phenolic, Heat Cured	Bloomingdale Rubber	<0	Aluminum	0.015	0.67	340	25
HT-424[2,3]	Epoxy Phenolic, Heat Cured	Bloomingdale Rubber	<0	Aluminum	0.015	0.67	340	25
HT-424 u[2,4]	Epoxy Phenolic, Heat Cured	Bloomingdale Rubber	<0	Aluminum	0.015	0.67	340	25

1. Similar to DuPont Adiprene L-100
2. Similar to Shell Epon 422J
3. Adhesive contains a fiberglass "Scrim Cloth" layer (See Figure 3.)
4. Contains no Scrim Cloth

27

TABLE II

DATA FOR GAS PERMEABILITY SPECIMENS

Adhesive/ Sample		Hole Diameter, Inches	Bond Overlap, Inches	Bond Thickness, Inches	H_2 Flow cc(STP)/Sec.	H_2 Permeability, SPU[1] (Reruns)	He Flow, cc(STP)/Sec.	He Permeability, SPU[1]
Narmco A/1	1	0.5	1.5	0.018	5.90×10^{-11}	5.3×10^{-12}		
	2	0.5	1.5	0.018	2.95×10^{-11}	$2.6 \times 10^{-12}(2.7 \times 10^{-12})$	3.2×10^{-10}	2.9×10^{-11}
	3	1.5	1.0	0.010	1.92×10^{-11}	$1.3 \times 10^{-11}(1.2 \times 10^{-12})$	7.0×10^{-10}	4.9×10^{-11}
	4	1.5	1.0	0.015	8.10×10^{-11}	$3.8 \times 10^{-12}(1.6 \times 10^{-11})$	2.7×10^{-9}	1.3×10^{-10}
	5	2.0	0.75	0.006	6.67×10^{-11}	5.1×10^{-12}	2.4×10^{-9}	1.8×10^{-10}
	6	2.0	0.75	0.007	8.56×10^{-11}	5.7×10^{-12}	2.7×10^{-9}	1.8×10^{-10}
	7	3.0	0.25	0.004	6.54×10^{-11}	2.1×10^{-12}	1.0×10^{-9}	3.2×10^{-11}
	8	3.0	0.25	0.004	1.06×10^{-10}	$3.4 \times 10^{-12}(1.3 \times 10^{-11})$	1.3×10^{-9}	4.1×10^{-11}
FM-1000/	1	0.5	1.5	0.007	4.42×10^{-9}	1.0×10^{-9}	3.1×10^{-8}	7.1×10^{-9}
	2	0.5	1.5	0.005	1.46×10^{-10}	$4.7 \times 10^{-11}(5.6 \times 10^{-11})$	3.1×10^{-8}	9.9×10^{-9}
	3	1.5	1.0	0.003	2.52×10^{-10}	5.9×10^{-11}	5.0×10^{-10}	1.2×10^{-10}
	4	1.5	1.0	0.003	5.08×10^{-10}	1.2×10^{-10}	3.6×10^{-10}	8.4×10^{-11}
	5	2.0	0.75	0.003	2.83×10^{-10}	$4.4 \times 10^{-11}(5.0 \times 10^{-11})$	1.0×10^{-10}	1.5×10^{-11}
	6	2.0	0.75	0.003	1.72×10^{-10}	2.6×10^{-11}	3.9×10^{-9}	6.0×10^{-10}
	7	3.0	0.25	0.001	4.35×10^{-10}	$5.5 \times 10^{-11}(6.1 \times 10^{-11})$	9.9×10^{-9}	1.3×10^{-9}
	8	3.0	0.25	0.003	9.45×10^{-10}	$4.0 \times 10^{-11}(2.2 \times 10^{-11})$	6.3×10^{-9}	2.7×10^{-10}
Narmco C/1	1	0.5	1.5	0.004	5.45×10^{-8}	2.2×10^{-8}	1.3×10^{-8}	5.2×10^{-9}
	2	0.5	1.5	0.008	6.80×10^{-9}	1.4×10^{-9}	2.3×10^{-10}	4.6×10^{-11}
	3	0.5	1.5	0.007	2.36×10^{-10}	5.4×10^{-11}	2.1×10^{-9}	4.8×10^{-10}
	4	1.5	1.0	0.011	2.06×10^{-10}	$1.3 \times 10^{-11}(6.4 \times 10^{-12})$	6.4×10^{-9}	4.1×10^{-10}
	5	1.5	1.0	0.009	2.29×10^{-10}	$1.8 \times 10^{-11}(1.6 \times 10^{-11})$	7.6×10^{-10}	5.9×10^{-11}
	6	2.0	0.75	0.008	6.75×10^{-10}	$3.9 \times 10^{-10}(4.6 \times 10^{-11})$	1.1×10^{-9}	6.4×10^{-11}
	7	2.0	0.75	0.006	5.06×10^{-10}	$3.9 \times 10^{-11}(4.6 \times 10^{-11})$	7.2×10^{-10}	5.5×10^{-11}
	8	3.0	0.25	0.003	3.38×10^{-10}	1.4×10^{-11}	1.2×10^{-8}	5.1×10^{-10}
	9	3.0	0.25	0.003	1.11×10^{-9}	4.7×10^{-11}		
BR-92/	1	0.5	1.5	0.007	8.83×10^{-11}	$2.0 \times 10^{-11}(1.6 \times 10^{-11})$	1.2×10^{-7}	2.7×10^{-8}
	2	0.5	1.5	0.007	6.73×10^{-7}	$2.7 \times 10^{-7}(Note2)$	5.0×10^{-8}	2.0×10^{-8}
	3	1.5	1.0	0.003	3.78×10^{-10}	$8.8 \times 10^{-11}(9.1 \times 10^{-11})$	2.7×10^{-8}	6.2×10^{-9}
	4	1.5	1.0	0.003	4.13×10^{-10}	9.6×10^{-11}		
	5	2.0	0.75	0.003	3.33×10^{-10}	$5.1 \times 10^{-11}(3.8 \times 10^{-11})$	8.7×10^{-9}	1.3×10^{-9}
	6	2.0	0.75	0.004	3.54×10^{-9}	4.1×10^{-10}		
	7	3.0	0.25	0.003	1.72×10^{-10}	7.3×10^{-12}	4.0×10^{-10}	1.7×10^{-11}
	8	3.0	0.25	0.003	2.99×10^{-10}	1.3×10^{-11}	2.1×10^{-9}	8.9×10^{-11}
X-424/	1	0.5	1.5	0.007	8.97×10^{-5}	2.1×10^{-5}	See note 3	3.1×10^{-5}
	2	1.5	1.0	0.006	2.72×10^{-3}	3.2×10^{-4}		5.0×10^{-3}
	3	2.0	0.75	0.006	2.09×10^{-5}	1.6×10^{-6}		2.0×10^{-6}
	4	3.0	0.25	0.005	1.21×10^{-3}	3.1×10^{-5}		2.0×10^{-5}
HT-424/	1	0.5	1.5	0.005	1.70×10^{-3}	5.5×10^{-4}		1.2×10^{-3}
	2	0.5	1.5	0.005	2.22×10^{-4}	7.1×10^{-5}		3.7×10^{-4}
	3	0.5	1.5	0.005	1.62×10^{-3}	5.2×10^{-4}		3.0×10^{-3}
	4	1.5	1.0	0.005	1.02×10^{-3}	1.4×10^{-4}		
	5	1.5	1.0	0.005	8.88×10^{-6}	1.2×10^{-6}		1.0×10^{-5}
	6	2.0	0.75	0.005	5.14×10^{-4}	4.7×10^{-5}		2.3×10^{-4}
	7	2.0	0.75	0.005	8.03×10^{-4}	7.4×10^{-5}		4.2×10^{-3}
	8	3.0	0.25	0.005	2.35×10^{-6}	6.0×10^{-8}		3.1×10^{-6}
	9	3.0	0.25	0.005	6.05×10^{-6}	1.5×10^{-7}		4.0×10^{-7}
HT-424u/	1	0.5	1.5	0.004	1.69×10^{-8}	6.8×10^{-9}		3.4×10^{-6}
	2	0.5	1.5	0.004	$>1.30 \times 10^{-2}$	$>5.2 \times 10^{-3}$		4.9×10^{-3}
	3	1.5	1.0	0.006	3.32×10^{-3}	3.9×10^{-4}		1.1×10^{-3}
	4	1.5	1.0	0.005	$>1.30 \times 10^{-2}$	$>1.8 \times 10^{-3}$		2.5×10^{-3}
	5	2.0	0.75	0.006	$>1.30 \times 10^{-2}$	$>1.0 \times 10^{-4}$		
	6	2.0	0.75	0.005	$>1.30 \times 10^{-2}$	$>1.3 \times 10^{-3}$		3.5×10^{-3}
	7	3.0	0.25	0.004	$>1.30 \times 10^{-2}$	$>4.1 \times 10^{-4}$		2.6×10^{-3}
	8	3.0	0.25	0.003	6.39×10^{-4}	2.7×10^{-5}		5.1×10^{-5}
Aerobond 430/	1	0.5	1.5	0.007	$>1.30 \times 10^{-2}$	$>3.0 \times 10^{-3}$		3.0×10^{-3}
	2	0.5	1.5	0.005	2.54×10^{-3}	8.2×10^{-4}		4.3×10^{-3}
	3	0.5	1.5	0.005	$>1.30 \times 10^{-2}$	$>4.2 \times 10^{-3}$		4.2×10^{-3}
	4	1.5	1.0	0.005	5.57×10^{-3}	6.5×10^{-4}		2.6×10^{-3}
	5	1.5	1.0	0.005	$>1.30 \times 10^{-2}$	$>1.5 \times 10^{-3}$		
	6	2.0	0.75	0.005	$>1.30 \times 10^{-2}$	$>1.2 \times 10^{-3}$		
	7	2.0	0.75	0.005	$>1.30 \times 10^{-2}$	$>1.2 \times 10^{-3}$		
	8	3.0	0.25	0.005	1.62×10^{-3}	4.1×10^{-5}		2.6×10^{-4}
	9	0.5	1.5	0.005	$>1.30 \times 10^{-2}$	$>4.2 \times 10^{-3}$		2.5×10^{-2}
	10	3.0	0.25	0.005	$>1.30 \times 10^{-2}$	$>3.3 \times 10^{-4}$		

(1) $1 SPU = 1 \, cm^3 \, (STP) \cdot sec^{-1} \cdot cm \cdot cm^{-2} \cdot (cm \, Hg \, \Delta P)^{-1}$
(2) Rerun indicated broken bond
(3) Where He flow rates are shown, flow and permeability data are from Veeco helium mass spectrometer leak detector; He permeabilities where no He flow is shown are from the Major A-6 volumetric apparatus.

TABLE III

DATA FOR LH$_2$ PERMEABILITY SPECIMENS

Material/Cell No.	Total Adhesive Thickness (in.)	Permeability cc(STP) . sec^{-1} . cm .cm^{-2} . (cm Hg ΔP)$^{-1}$					
		LH$_2$ Run 1	LH$_2$ Run 2	LH$_2$ Run 3	GHe (before LH$_2$)	GH$_2$ (before LH$_2$)	GH$_2$ (after LH$_2$)
FM-1000/ 1	0.0877	>1.80 x 10^{-5}(1)	-	-	9.45 x 10^{-12}	-	-
2	0.1422	<1.88 x 10^{-10}	<1.88 x 10^{-10}	<1.88 x 10^{-10}	-	8.1 x 10^{-10}	<1.88 x 10^{-10}
3	0.1724	<1.55 x 10^{-10}	<1.55 x 10^{-10}	<1.55 x 10^{-10}	-	-	<1.55 x 10^{-10}
BR-92/ 1	0.1501	<1.77 x 10^{-10}	ruptured during LN$_2$ precool	-	7.65 x 10^{-12}	-	-
2	0.1613	>9.8 x 10^{-6}(1)	-	-	1.24 x 10^{-11}	-	-
3	0.1396	<1.91 x 10^{-10}	>1.3 x 10^{-5}(1)	-	-	-	-
Narmco A/ 1	0.2485	<1.07 x 10^{-10}	<1.07 x 10^{-10}	<1.07 x 10^{-10}	2.82 x 10^{-11}	-	<1.07 x 10^{-10}
2	0.3594	<7.45 x 10^{-11}	<7.45 x 10^{-11}	<7.45 x 10^{-11}	-	-	<7.45 x 10^{-11}
3	0.2492	>1.07 x 10^{-10}	ruptured during LN$_2$ precool	-	-	-	-
Narmco C/ 1	0.1895	<1.41 x 10^{-10}	>8.33 x 10^{-6}(1)	-	2.97 x 10^{-12}	2.2 x 10^{-11}(2)	-
2	0.1521	<1.76 x 10^{-10}	>1.04 x 10^{-5}(1)	-	2.97 x 10^{-12}	-	-
3	0.0301	<8.87 x 10^{-9}	>5.25 x 10^{-5}(1)	-	-	-	-

(1) Pressure and H$_2$ level indicated adhesive fracture during run.

(2) Veeco sensitivity was higher at room temperatures than for LH$_2$ tests.

TABLE IV

PERMEABILITY TO LIQUID NITROGEN AND AIR

Material	Cell No.	Total Adhesive Thickness, in.	Permeability cc(STP)$\cdot$sec$^{-1}\cdot$cm$\cdot$cm$^{-2}\cdot$(cm Hg ΔP)$^{-1}$	
			$\underline{LN_2}$	$\underline{Air}$
Aerobond 430	1	0.652	6.7×10^{-2}	7.0×10^{-2}
	2	0.647	1.2×10^{-1}	1.4×10^{-1}
HT-424	1	0.892	1.2×10^{-2}	2.3×10^{-2}
	2	0.904	4.1×10^{-3}	3.4×10^{-3}

PERMEATION OF ADHESIVELY BONDED JOINTS
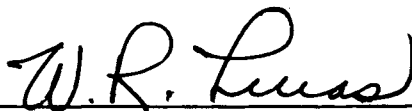## BY GASEOUS AND LIQUID HYDROGEN

By

C. T. Egger
D. A. Nauman
T. J. Carter
J. B. Gayle

The information in this report has been reviewed for security classification. Review of any information concerning Department of Defense or Atomic Energy Commission programs has been made by the MSFC Security Classification Officer. This report, in its entirety, has been determined to be unclassified.

This document has also been reviewed and approved for technical accuracy.

_____

W. A. RIEHL
Chief, Chemistry Branch

_____

W. R. LUCAS
Chief, Materials Division

_____

F. B. CLINE
Acting Director, Propulsion & Vehicle Engineering Laboratory

31

DISTRIBUTION

R-P&VE-DIR   Mr. Cline
R-P&VE-DIR   Mr. Palaoro
R-P&VE-V   Mr. Aberg
R-P&VE-S   Mr. Kroll
R-P&VE-P   Mr. Paul
R-P&VE-M   Dr. Lucas (5)
R-P&VE-MN   Mr. Shannon (3)
R-P&VE-MM   Mr. Cataldo
R-P&VE-ME   Mr. Kingsbury
R-P&VE-MC   Mr. Riehl (25)
R-RP-DIR   Dr. Stuhlinger
R-ME-M   Mr. Orr (2)
R-QUAL-DIR   Mr. Grau
R-ASTR-DIR   Dr. Haeussermann
R-AERO-ES   Mr. Ballance
R-TEST-C   Mr. Connor
R-P&VE-RT   Mr. Hofues
MS-H   Mr. Akens
MS-IP   Mr. Remer
MS-IPL   Miss Robertson (8)
CC-P   Mr. Wofford
MS-T   Mr. Wiggins

Douglas Aircraft Company, Incorporated
Materials Research & Production Methods
Huntington Beach, California
Attention: Mr. R. L. Long
            Mr. R. F. Zemer
            Mr. G. Bryan
            Mr. R. A. Kallas

North American Aviation, Incorporated
Space and Information Systems Division
Downey, California
Attention: Mr. B. Healy
            Mr. J. O. Laws
            Mr. D. Simkin
            Mr. D. Drysol

DISTRIBUTION (Concluded)

General Electric Company
Valley Forge Space Technology Center
P. O. Box 8555
Philadelphia, Pennsylvania
Attention: Mr. Carl P. Boebel, Materials Evaluation
M&P Engineering, Room 4223-U

National Aeronautics and Space Administration
Lewis Research Center
21000 Brookpark Road
Cleveland, Ohio 44135

National Aeronautics and Space Administration
Washington, D. C. 20546
Attention: Bernard Achhammer, RRM

Scientific and Technical Information Facility (25)
(S-AK/RKT)
P. O. Box 5700
Bethesda, Maryland